



Receptor for Advanced Glycation End Products (RAGE) Mediates Cognitive Impairment Triggered by Pneumococcal Meningitis

Vijayasree V. Giridharan¹ · Jaqueline S. Generoso² · Allan Collodel² · Diogo Domingui² · Cristiano Julio Faller² · Flavio Tardin² · Gursimrat S. Bhatti¹ · Fabricia Petronillo³ · Felipe Dal-Pizzol² · Tatiana Barichello^{1,2} 

Published online: 4 September 2020

© The American Society for Experimental NeuroTherapeutics, Inc. 2020

Abstract

Pneumococcal meningitis is a life-threatening infection of the central nervous system (CNS), and half of the survivors of meningitis suffer from neurological sequelae. We hypothesized that pneumococcal meningitis causes CNS inflammation via the disruption of the blood–brain barrier (BBB) and by increasing the receptor for advanced glycation end product (RAGE) expression in the brain, which causes glial cell activation, leading to cognitive impairment. To test our hypothesis, 60-day-old Wistar rats were subjected to meningitis by receiving an intracisternal injection of *Streptococcus pneumoniae* or artificial cerebrospinal fluid as a control group and were treated with a RAGE-specific inhibitor (FPS-ZM1) in saline. The rats also received ceftriaxone 100 mg/kg intraperitoneally, bid, and fluid replacements. Experimental pneumococcal meningitis triggered BBB disruption after meningitis induction, and FPS-ZM1 treatment significantly suppressed BBB disruption. Ten days after meningitis induction, surviving animals were free from infection, but they presented increased levels of TNF- α and IL-1 β in the prefrontal cortex (PFC); high expression levels of RAGE, amyloid- β (A β _{1–42}), and microglial cell activation in the PFC and hippocampus; and memory impairment, as evaluated by the open-field, novel object recognition task and Morris water maze behavioral tasks. Targeted RAGE inhibition was able to reduce cytokine levels, decrease the expression of RAGE and A β _{1–42}, inhibit microglial cell activation, and improve cognitive deficits in meningitis survivor rats. The sequence of events generated by pneumococcal meningitis can persist long after recovery, triggering neurocognitive decline; however, RAGE blocker attenuated the development of brain inflammation and cognitive impairment in experimental meningitis.

Key Words Pneumococcal meningitis · RAGE · amyloid- β · blood–brain barrier · inflammation · cognition

Vijayasree V. Giridharan and Jaqueline S. Generoso contributed equally to this work.

✉ Tatiana Barichello
Tatiana.Barichello@uth.tmc.edu

¹ Translational Psychiatry Program, Department of Psychiatry and Behavioral Sciences, McGovern Medical School, The University of Texas Health Science Center at Houston, 1941 East Road, Houston, TX 77054, USA

² Laboratory of Experimental Pathophysiology, Graduate Program in Health Sciences, University of Southern Santa Catarina (UNESC), Criciúma 88806-000, SC, Brazil

³ Laboratory of Neurobiology of Inflammatory and Metabolic Processes, Graduate Program in Health Sciences, Health Sciences Unit, University of South Santa Catarina, Tubarão 88704-900, SC, Brazil

Introduction

Pneumococcal meningitis is a life-threatening infection of the central nervous system (CNS) with a case-fatality rate ranging from 10 to 40% [1–3]. A high rate of neurological sequelae was estimated to occur in 30 to 55% of meningitis survivors [4, 5]. *Streptococcus pneumoniae* enters the cerebrospinal fluid (CSF) through the subarachnoid space by crossing the blood–brain barrier (BBB) or the choroid plexus blood–CSF barrier (BCSFB) or through an adjacent site of infection [6, 7]. The invading pathogen multiplies and releases bacterial compounds that are highly immunogenic, and the pattern recognition receptors (PRRs) recognize these bacterial components, leading to the activation of the host immune response, thereby increasing the disease severity [8].

The receptor for advanced glycation end products (RAGE) is a multiligand transmembrane receptor that initiates several immune pathways and triggers the migration and activation of

immune cells [9]. RAGE is expressed in a variety of cells, including endothelial cells, microglia [10], and astrocytes [11], and can be activated by some ligands, such as advanced glycation end products (AGEs), amyloid- β (A β), and high mobility group box-1 (HMGB-1) protein. RAGE mediates A β peptide transference through the BBB, facilitating its deposition in the brain, which is a critical risk factor for Alzheimer's disease (AD) [12]. Also, RAGE contributes to the transport of A β from the cell surface to the intracellular space, thereby increasing A β toxicity and causing neuronal dysfunction [13]. RAGE levels are low under homeostasis but are highly expressed under inflammatory states when the levels of various RAGE ligands are increased [14]. Because RAGE plays an essential role in the pathogenesis of several infectious and inflammatory diseases [14, 15], in this research project, we aimed to explore the inhibition of the RAGE receptor by FPS-ZM1 in an experimental pneumococcal meningitis model and to characterize the neuroprotective effects of FPS-ZM1 as well as prevention of BBB disruption and cognitive impairment by FPS-ZM1.

Materials and Methods

Preparation of *S. pneumoniae* for Meningitis Induction

The strain of serotype III *S. pneumoniae* was purchased from Microbiologics (ATCC 6303), St Cloud, MN 56303. It was cultured in 5 mL of Todd Hewitt Broth BBL™. The microorganism was then diluted in fresh medium and allowed to grow to the logarithmic phase. The culture was centrifuged for 10 min at 1200 rpm and resuspended in sterile pyrogen-free saline to a concentration of 5×10^9 colony-forming units (CFU) [16].

Animal Model of Meningitis

Male Wistar rats (8 weeks old) weighing 200 to 250 g were purchased from Charles River and housed at a temperature of 20 ± 2 °C and a humidity level of 30% on a 12-h light–dark cycle (lights on 06:00 hours). Food and water were available *ad libitum*. All protocols were approved by the Institutional Animal Welfare Committee of the Center for Laboratory Animal Medicine and Care (CLAMC) of the University of Texas Health Science Center at Houston (UTHealth), TX, USA (AWC-16-0106). The rat under anesthesia (2.5% vapor concentration in O₂) was placed in the center of the stereotaxic apparatus, and the fixation bar was attached to the ears. The preparation of the injection site was done by clipping the hair from the injection site and disinfection of the skin using chlorhexidine or povidone–iodine. The position of the head was adjusted until an angle of approximately 110° was reached

between the base of the stereotaxic and the snout of the rat. This position allowed the easy identification of the cisterna magna, which has a depressed rhomboid area between the occipital protuberance and the spine [17]. The stereotaxic coordinates used were A–P, -1.5 ± 1 mm, and M–L, 0 mm. The D–V coordinate was not used, as the coordinates A–P and M–L were adequate to identify the puncture site. The coordinates were obtained from the stereotaxic zero point, which is defined as a point where the 2 centralized ear bars meet [17]. A precise aspiration was performed so that the colorless CSF would flow through the needle to avoid any possible blood contamination [18]. The sham control and meningitis rats received an intracisternal (i.c.) injection of 10 μ L of artificial CSF (aCSF, Tocris Bioscience, Bristol, UK) as a placebo and an equivalent volume of the serotype III *S. pneumoniae* suspension, respectively. Eighteen hours after meningitis induction or aCSF inoculation, meningitis was confirmed by incubating a quantitative culture of 5 μ L of CSF at 35 °C with 5% CO₂ in sheep blood agar [19], and afterward, the animals received ceftriaxone (100 mg/kg, i.p., for 7 days) twice a day [20]. The rats were also given buprenorphine 1 mL/kg as an analgesic.

Experimental Design

After acclimatization, the rats were randomly divided into 4 different groups: control/saline, control/FPS-ZM1, meningitis/saline, and meningitis/FPS-ZM1. FPS-ZM1 was procured from Millipore Sigma, MA (Cat no. 553030). The first experiment involves the treatment of the animals with an intraperitoneal (i.p.) injection of 1.5 mg/kg of FPS-ZM1 or saline immediately after meningitis induction or aCSF inoculation [21]. The animals were then injected with Evan's blue into the femoral vein to investigate BBB integrity [22] 1 h before being euthanized at 12, 18, and 24 h after meningitis induction and FPS-ZM1 administration [21]. The animals did not receive antibiotic treatment.

In the second experiment, the animals submitted to behavioral tests received intraperitoneal injections of 1.5 mg/kg of FPS-ZM1 or saline from day 1 to day 5 [21], and the animals also received ceftriaxone (100 mg/kg, i.p., for 7 days) twice a day. A separate cohort of animals was subjected to an open-field task, a novel object recognition task (NORT), and a Morris water maze. On day 10, after the behavioral study, the rats were euthanized using 4 to 5% isoflurane. For biochemical evaluation, the brain was dissected, and the prefrontal cortex (PFC) and hippocampus were immediately isolated and stored at -80 °C until further processing. Note: After validating that the control/saline and control/FPS-ZM1 groups did not present statistically significant differences in the Morris water maze (MWM) task, we removed the latter group from the open field and NORT to decrease the number of animals. The schematic diagram of the experimental design is given in Fig. 1a.

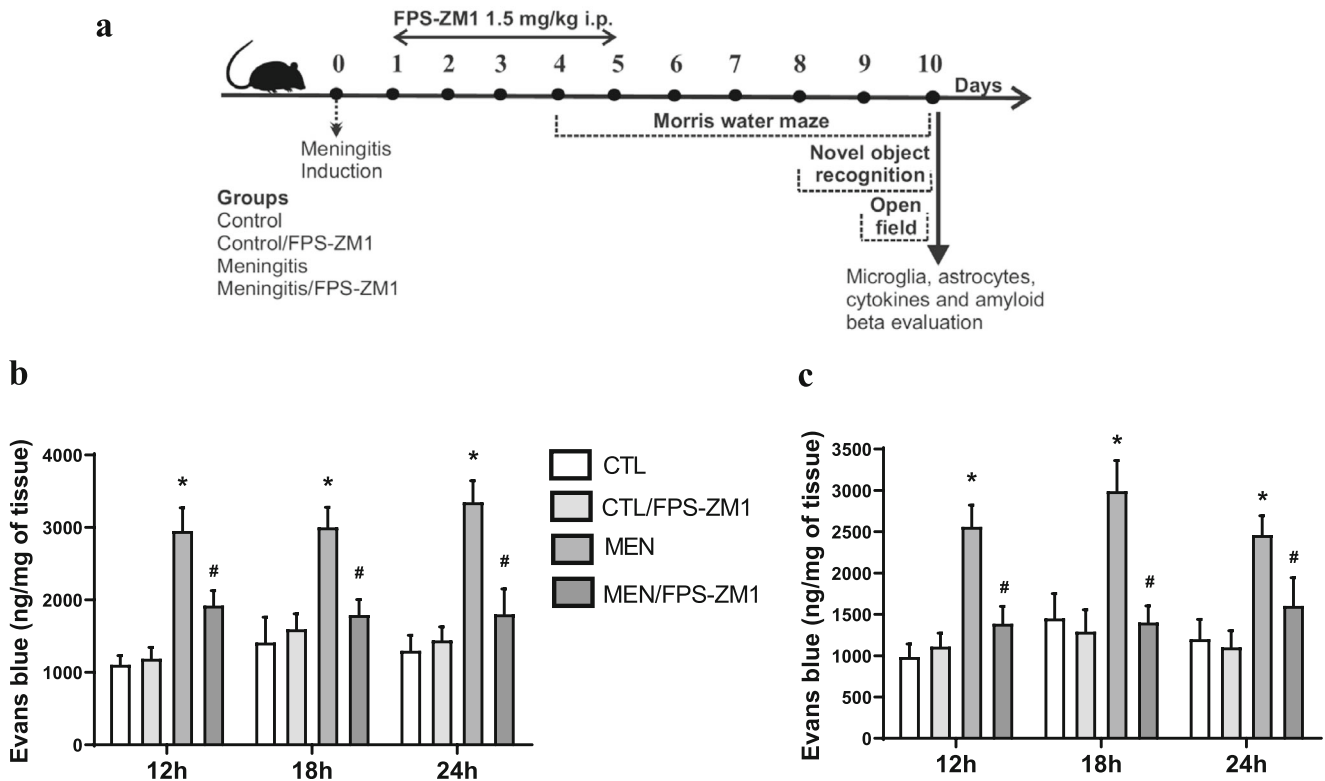


Fig. 1 (a) Schematic diagram of the experimental design. The integrity of the blood-brain barrier (BBB) in the cerebral cortex (b) and hippocampus (c) was obtained several times at 12, 18, and 24 h after meningitis induction. Results show the mean \pm SEM of animals ($n = 6$) in each group

determined by 2-way ANOVA and Tukey's test. * $p < 0.05$ indicates statistical significance compared to the control group; # $p < 0.05$ indicates statistical significance when compared to the meningitis group

Behavioral Study

Open-Field Task

The apparatus was a 40×60 -cm open field surrounded by 50-cm-high dark gray walls and a front glass wall. Black lines divided the floor of the open field into 9 rectangles. Each animal was gently placed in the center of the open field and was left to explore the arena for 5 min (training session). The number of crossings (the number of times that the animal crossed the black lines, an assessment of locomotor activity) and rearing movements (exploratory behavior observed in rats subjected to a new environment) were measured. Immediately after this procedure, the animals were taken back to their home cage. Twenty-four hours later, the animals were subjected to a training session, and the number of times the animal crossed the black lines or reared was counted during a 5-min period. The reduction in the number of crossings and rearings between the 2 sessions was taken as a measure of the retention of memory. The behavioral test was conducted by a person who was blinded to the group treatments [23].

Novel Object Recognition Task

This task evaluates nonaversive and nonspatial memory. The same apparatus used for the open-field task was used for the

NORT. All animals were subjected to a habituation session in which they were allowed to freely explore the open field for 5 min; no objects were placed in the box during the habituation trial. The number of times the black lines were crossed and the number of rearings that occurred in this session were used as indicators of locomotor and exploratory activity, respectively. Two identical objects (objects A1 and A2, both cubes) were placed in 2 adjacent corners, 10 cm from the walls. In the long-term recognition memory test that was given 24 h after training, the rats explored the open field for 5 min in the presence of 1 familiar object (A) and 1 novel object (B), a pyramid with a square-shaped base. All of the objects were similar in texture, color, and size but were distinctive in shape. A recognition index was calculated for each animal and reported as the ratio $TB/(TA + TB)$, where TA = time spent exploring the familiar object A and TB = time spent exploring the novel object B. Recognition memory was evaluated as in the long-term memory test. Exploration was defined as sniffing or touching the object with the nose or forepaws.

Morris Water Maze

A spatial memory test was performed using the MWM [24]. The MWM is performed in a circular pool with a diameter of 170 cm and a wall height of 65 cm. Briefly, the pool was filled

with water to approximately 35 cm high, a platform (12.5 cm diameter and 33 cm height) was kept in the pool, and the temperature of the water was maintained at 20 ± 2 °C to avoid hypothermia. A camera connected to a computer was kept above the pool to record the movement of the animal. The pool was divided into 4 equal quadrants (I, II, III, and IV), and a platform was kept in IV or a target quadrant. All rats were given 4 trials each day during daily acquisition sessions across 4 days. A trial started as soon as the rats were placed in the tank, facing the walls. Each of the 4 starting points was used once in a series of trials. The position of the platform was not changed during the trial. The trial comes to an end as soon as the rat reaches the platform or when 120 s elapses. The rats were allowed to stay on the platform for 5 s. If the rats were not able to find the platform within 120 s, they were guided to the platform gently and allowed to stay there for 10 s. The rats were then gently dried with a clean towel and returned to the home cage after each trial. The time the rats took to reach the platform was noted in all the trials. On the fifth day, a probe trial or retention trial was carried out to detect the spatial memory of the rats. The hidden platform was removed from the tank, and the rats were given 120 s to swim and find the platform. A record of the time spent swimming in the pool quadrant in which the platform had been previously placed was recorded.

Biochemical Evaluation

Blood–Brain Barrier Permeability by Evan’s Blue Dye

The BBB integrity was investigated using Evan’s blue dye extravasations [22]. One hour before euthanization, 1% of 1 mL of Evan’s blue dye was injected into the femoral vein. The chest was subsequently opened and transcardially perfused with 200 mL of saline through the left ventricle at 100 mmHg pressure until colorless perfusion fluid was obtained from the right atrium. The brain was weighed and placed in a 50% trichloroacetic solution. Following homogenization and centrifugation, the extracted dye was diluted with ethanol (1:3), and its fluorescence was determined (excitation at 620 nm and emission at 680 nm) using a luminescence spectrophotometer (Hitachi 650-40, Tokyo, Japan). Calculations were based on the external standard (62.5–500 ng/mL) with the same solvent. The tissue containing Evan’s blue dye was quantified with a standard linear line derived from known amounts of the dye and was expressed per gram of tissue [22]. BBB permeability was measured at 12, 18, and 24 h after pneumococcal meningitis induction.

Assessment of Cytokine Levels

The animals were euthanized, and the PFC and hippocampus were removed for the evaluation of TNF- α , IL-1 β , IL-6, and

IL-10 levels. Briefly, the hippocampus and PFC were homogenized in extraction solution containing aprotinin (100 mg of tissue per 1 mL) containing 0.4 mol/L NaCl, 0.05% Tween 20, 0.5% 7 BSA, 0.1 mmol/L phenyl methyl sulfonyl fluoride, 0.1 mmol/L benzethonium chloride, 10 mmol/L EDTA, and 20 KI aprotinin using Ultra-Turrax (Fisher Scientific, Pittsburgh, PA). The concentrations of cytokines/chemokines in the PFC and hippocampus were determined using commercially available ELISA assays, following the instructions supplied by the manufacturer (DuoSet kits, R&D Systems, Minneapolis, MN). The results were reported in picograms/100 mg in the PFC and hippocampal tissue. Protein was measured using the method of Lowry et al. (1951) using bovine serum albumin as a standard [25].

Western Blot Analysis

Western blot analysis was performed as per the protocols of the previous studies [26]. The PFC and hippocampus regions of the brain were thawed and homogenized using Complete Protease Inhibitor Cocktail tablets (Roche Diagnostics, Indianapolis, IN). Then, the homogenate was centrifuged at 12,000 rpm for 20 min at 4 °C. A bicinchoninic acid (BCA) assay was used to determine the protein concentrations in the tissue. For the Western blot run, equal amounts of protein (30–50 μ g) for each sample were loaded in Mini-Protean TGX precast gels (Bio-Rad, Hercules, CA). Proteins were transferred onto polyvinylidene difluoride (PVDF) membranes using a Trans-Blot® Turbo™ system (Bio-Rad). The PVDF membranes were blocked with 5% nonfat dry milk (Bio-Rad) in Tris-buffered saline plus 0.1% Tween 20 buffer (TBST, Bio-Rad) for 1 h at room temperature (RT) and kept overnight in a cold room on a shaker with primary antibodies. The primary antibodies used were A β (1:1000, Abcam, ab62658), GFAP (1:1000, Abcam, ab7260), CD11B (1:1000, Abcam, ab75476), CD68 (1:1000, Abcam, ab201340), HMGB-1 (1:1000, Abcam, ab18256), RAGE (1:1000, Abcam, ab216329), IBA-1 (1:2000, ab108539), and NLRP3 (1:1000, Novus, NBP2-12446). The following day, the blots were washed 3 times in TBST and incubated with a horseradish peroxidase-conjugated secondary antibody (1:10,000) for 1 h at RT. The blots were washed 3 times for 10 min using TBST; then, the bands were detected using enhanced chemiluminescence (Clarity Western ECL Substrate; Bio-Rad) with the ChemiDoc MP (Bio-Rad) Western blotting imaging system. After imaging, the blots were incubated in a stripping buffer (Thermo Fisher Scientific 46430, Rockford, IL) for 10 to 15 min at RT, followed by 3 washes with TBST. The stripped blots were incubated in blocking solution (5% nonfat dry milk in TBST) for 60 min and then incubated with the primary antibody against β -tubulin (1:5000, Abcam, ab6046) as a loading control. The densitometric analysis of each protein was conducted using Image Lab™ software (Bio-Rad).

The results were expressed as the ratio between the loading control and the target protein.

Immunohistochemistry

For immunostaining, we used formalin-fixed, paraffin-embedded brain tissue samples. Deparaffinization and rehydration were carried out using a series of xylenes, graded alcohols, and reagent-grade water. Heat-based antigen retrieval was performed using a 1× antigen retrieval sodium citrate solution at pH 9 (Agilent Technologies, Santa Clara, CA) for 30 min at 95 °C, followed by 30 min on ice. Subsequent washing steps were carried out using a 1× phosphate-buffered saline solution (PBS) (Bio-Rad). A 3% hydrogen peroxide solution (VWR International, Radnor, PA) was used to block endogenous peroxidase for 10 min. The tissue sections were blocked at room temperature with 2.5% horse serum (Vector Laboratories, Burlingame, CA). Following the blocking step, primary antibodies for A β _(1–42) (Abcam, ab10148, 1:1000), IBA-1 (Abcam, ab178846, 1:1000), GFAP (Abcam, ab7260, 1:1000), and RAGE (Abcam, 216,329, 1:2000) were added and kept at 4 °C overnight. The next day, slides were washed with PBS, and goat anti-rabbit biotinylated secondary antibody (Millipore, Burlington, MA) was applied for 1 h at room temperature. Then, avidin–biotin complex (ABC) was added for 1 h. Following additional washing steps, the target antigen was visualized using DAB chromogen in substrate buffer (Vector, Burlingame, CA). For counterstaining, hematoxylin was applied, and slides were taken to xylene and mounted with Permount™ (Fischer Chemicals). The staining was visualized using Nikon ECLIPSE Ci-S (Nikon Instruments, Tokyo, Japan), and the images were captured (magnification, × 40).

Statistical Analysis

All data were submitted to normal (Gaussian) distribution using the Shapiro–Wilk normality test as a method to test the distribution. Data from open-field task groups were compared using the paired Student's *t* test (training and test) and 1-way analysis of variance (ANOVA) followed by Tukey's post hoc test which was used to compare the variables between groups. We also used the Kruskal–Wallis *H* (comparisons between groups) and Wilcoxon's tests (comparisons between training and the same group test). For the BBB, cytokines, MWM, Western blotting, and IHC, 2-way ANOVA and Tukey's test were used. The results are expressed as the mean ± SEM. Statistically significant results are indicated by **p* < 0.05. All statistical analyses were performed using GraphPad Prism 8.0 (GraphPad Software, Inc., La Jolla, CA).

Results

RAGE Inhibition Improves BBB Integrity

Figure 1b, c demonstrates the BBB integrity targeting RAGE inhibition in experimental pneumococcal meningitis in the cerebral cortex and hippocampus. Previously, we reported BBB breakdown at 12 h after pneumococcal meningitis induction [27]. In this study, RAGE inhibition prevented BBB breakdown at 12, 18, and 24 h after pneumococcal meningitis induction in the cerebral cortex (Fig. 1b, $F(3, 16) = 65.158$, $p < 0.001$; $F(3, 16) = 49.255$, $p < 0.001$; $F(3, 16) = 70.146$, $p < 0.001$, respectively) and hippocampus (Fig. 1c, $F(3, 15) = 32.372$, $p < 0.001$; $F(3, 15) = 38.606$, $p < 0.001$; $F(3, 15) = 30.797$, $p < 0.001$, respectively).

RAGE Inhibition Improves Cognitive Impairment

Pneumococcal meningitis triggers cognitive impairment [28], and in Figs. 2 and 3, we demonstrated whether RAGE inhibition improves cognitive impairment mediated by pneumococcal meningitis. At 10 days after meningitis induction, the animals were subjected to the open-field task to investigate habituation memory. The meningitis group did not show a difference in behavior between the training and test sessions. In contrast, the control groups demonstrated habituation memory by spending significantly less time exploring in the test session. However, RAGE inhibition prevented habituation memory impairment triggered by pneumococcal meningitis (Fig. 2a, $F(2, 24) = 2.641$, $p < 0.05$). Recognition memory was evaluated by subjecting the animals to the NORT. The more time the animal explores the novel object reveals improved learning and recognition memory. The meningitis group did not recognize the new object; however, the meningitis group treated with RAGE inhibitor spent more time exploring the new object placed in the field, demonstrating recognition memory (Fig. 2b, $p < 0.05$). The MWM task was utilized to test spatial memory after RAGE inhibitor treatment. We found no difference between groups during the training trial. However, in the probe trial, the time spent in the target quadrant was significantly reduced in the meningitis group rats. RAGE inhibition increased the time spent in the target quadrant and improved spatial memory in the meningitis group (Fig. 3, $F(3, 31) = 5.505$, $p < 0.003$).

RAGE Inhibition Reduces Cytokine Levels, Glial Activation, and Amyloid Expression

Further, we investigated the effect of RAGE inhibition on the levels of TNF- α , IL-1 β , IL-6, and IL-10 in the PFC and hippocampus at 10 days after pneumococcal meningitis induction as demonstrated in Fig. 4. The levels of TNF- α and IL-1 β in the PFC were higher than those of the control group (Fig. 4a, *F*

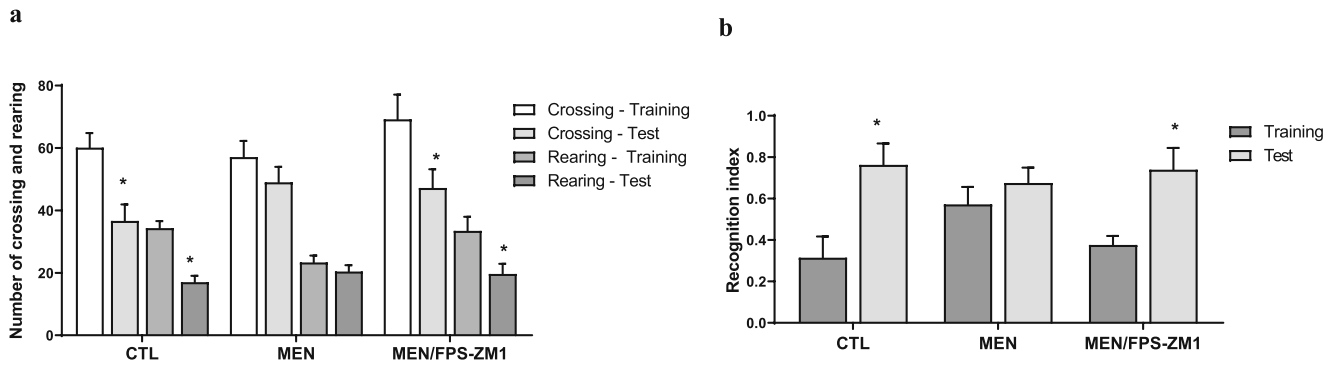


Fig. 2 (a) Effects of RAGE inhibition on habituation to the open field task in adult Wistar rats 10 days after pneumococcal meningitis induction. The numbers of crossings and rearing movements are reported as the mean ± SEM and were analyzed by the paired Student's *t* test [10]. **p* < 0.05 statistically different from the training session. (b) Novel object recognition test in Wistar rats 10 days after submission to pneumococcal

meningitis and treated or not with RAGE. Data were presented as median and interquartile range. Comparisons among groups for the object recognition test were performed using a Mann-Whitney *U* test. The intragroup comparisons were performed using Wilcoxon's tests (*n* = 10). **p* < 0.05 indicates statistically significant when compared to the training and test sessions

(3, 15) = 3.965, *p* < 0.05, and b *F* (3, 17) = 9.876, *p* < 0.05); however, targeted RAGE inhibition decreased the levels of these cytokines. In the hippocampus, RAGE inhibition increased IL-10 levels compared to those in the control group (Fig. 4d, *F* (3, 19) = 2.710, *p* < 0.05). Using the Western blot technique, we evaluated RAGE, Aβ₁₋₄₂, and HMGB-1 (RAGE ligands); CD11B (microglia and macrophage marker); GFAP (astrocyte marker); CD68 (monocyte, microglia, and tissue macrophage marker); and NLRP3 inflammasome (AGE ligands) in the PFC and hippocampus of animals submitted to pneumococcal meningitis as represented in Figs. 5 and 6. In the PFC, RAGE (*F* (3, 13) = 7.271, *p* < 0.004), Aβ₁₋₄₂ (*F* (3, 13) = 6.438, *p* < 0.006), CD11B (*F* (3, 13) = 6.248, *p* < 0.007), and CD68 (*F* (3, 12) = 5.154, *p* < 0.01) and expression levels increased at 10 days after meningitis induction; however, RAGE inhibition decreased the expression levels of RAGE (*p* < 0.01), Aβ₁₋₄₂ (*p* < 0.05), and CD68 (*p* < 0.05) levels (Fig. 5). The hippocampus showed high expression

levels of RAGE (*F* (3, 14) = 5.646, *p* < 0.009), Aβ₁₋₄₂, (*F* (3, 14) = 4.721, *p* < 0.01), CD11B (*F* (3, 14) = 4.404, *p* < 0.02), CD68 (*F* (3, 13) = 4.703, *p* < 0.01), and NLRP3 (*F* (3, 13) = 4.815, *p* < 0.01) compared to those in the control group; however, RAGE inhibitor treatment decreased the expression of RAGE, CD11B, and NLRP3 markers (Fig. 6, *p* < 0.05). Using the IHC technique, we localized and recognized protein markers for microglia (IBA-1), astrocytes (GFAP), RAGE, and Aβ₁₋₄₂ in the PFC and hippocampus 10 days after pneumococcal meningitis induction (Figs. 7, 8, 9, 10, 11, 12, 13, and 14). We found a higher number of cells immunostained for IBA-1 in the meningitis group than that in the control group in the PFC (*F* (3, 8) = 27.38, *p* < 0.0003) and hippocampus (*F* (3, 8) = 5.710, *p* < 0.02) (Figs. 7 and 8). However, RAGE inhibitor treatment decreased IBA-1 expression levels in both brain structures (Figs. 7 and 8). GFAP staining did not reveal differences among the groups (PFC, *F* (3, 8) = 3.095, and hippocampus *F* (3, 8) = 6.740, *p* < 0.40)

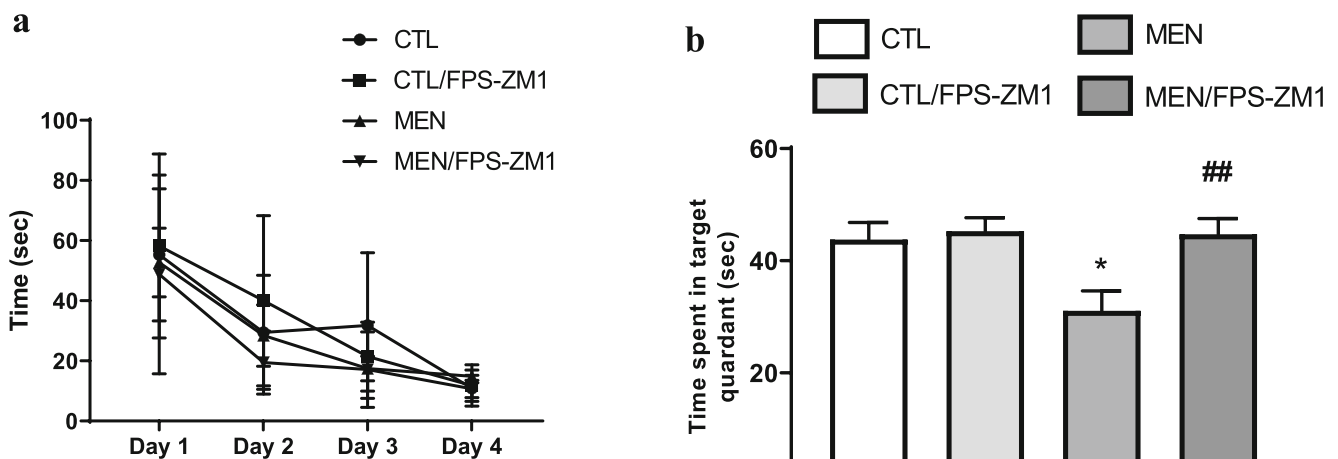


Fig. 3 Effects of RAGE inhibition on spatial memory using Morris water maze in adult Wistar rats 10 days after pneumococcal meningitis induction. Morris water maze training (a) and probe trial (b). **p* < 0.05

indicates statistical significance compared to the control group; #*p* < 0.05 indicates statistical significance when compared to the meningitis group (*n* = 8-10)

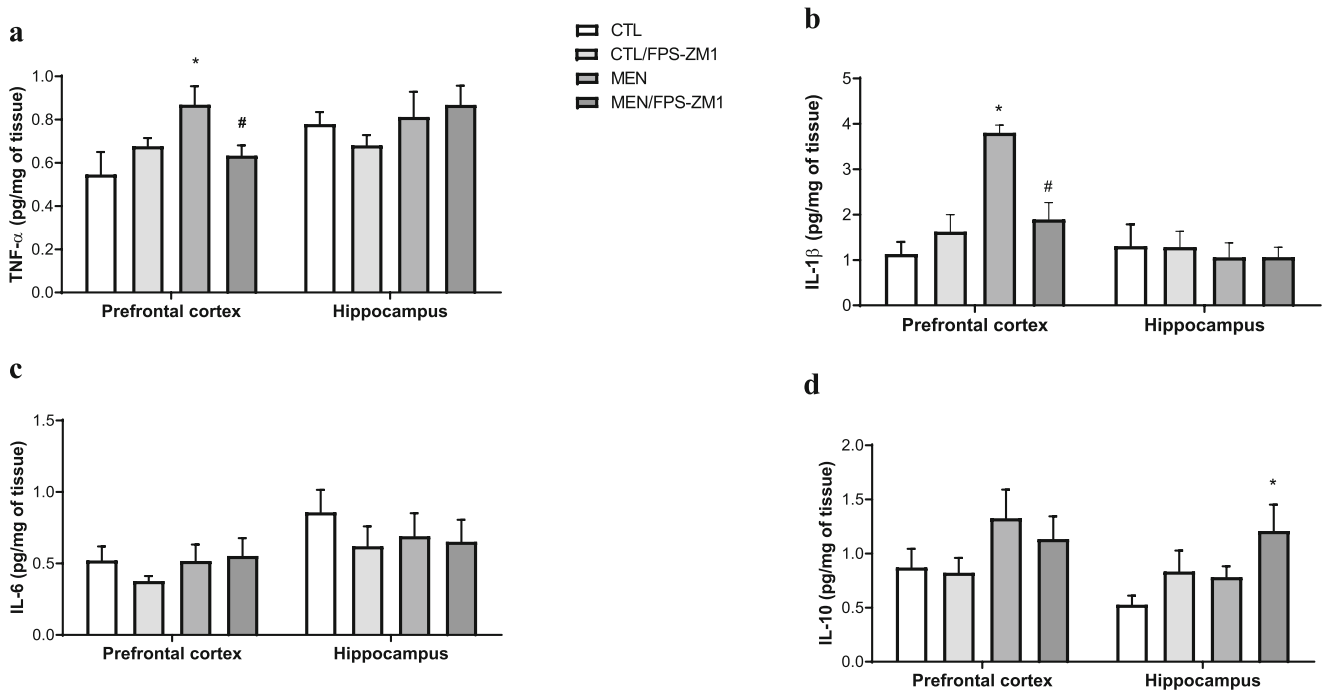


Fig. 4 Levels of TNF- α (a), IL-1 β (b), IL-6 (c), and IL-10 (d) in the prefrontal cortex and hippocampus of adult Wistar rats 10 days after submission to pneumococcal meningitis treated or not with RAGE

inhibitor. Data were presented as mean \pm SEM and analyzed by 2-way ANOVA. * $p < 0.05$; # $p < 0.05$ indicate statistical significance when compared to the meningitis group ($n = 5-6$)

(Figs. 9 and 10). RAGE immunostaining increased in the meningitis group compared with that in the control group in the PFC ($F(3, 8) = 51.78, p < 0.0001$) and hippocampus ($F(3, 8) = 19.42, p < 0.0005$) (Figs. 11 and 12). RAGE inhibitor treatment decreased RAGE immunostaining in both brain

structures compared to the meningitis group (Figs. 11 and 12). A β_{1-42} immunostaining increased in the meningitis group in both the PFC ($F(3, 8) = 20.41, p < 0.0004$) and hippocampus ($F(3, 8) = 13.63, p < 0.001$) brain structures compared with that in the control group (Figs. 13 and 14). As

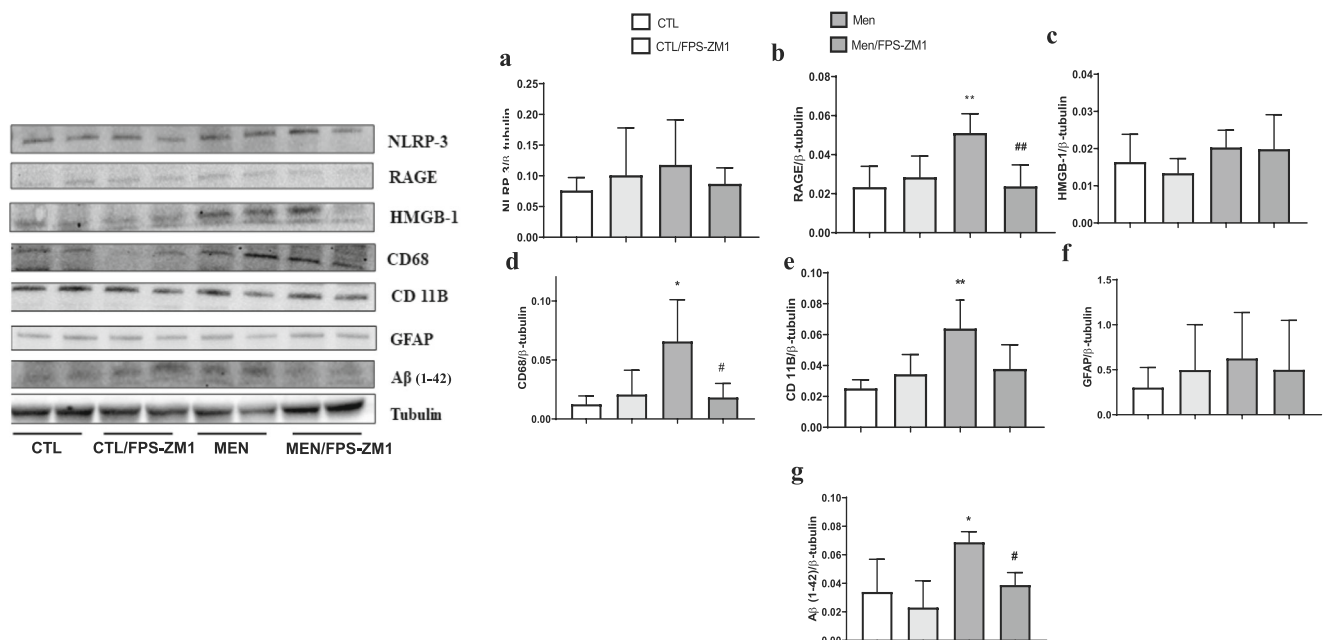


Fig. 5 Expression of NLRP3 (a), RAGE (b), HMGB1 (c), CD68 (d), CD11B (e), GFAP (f), and β -amyloid (g) in the prefrontal cortex of Wistar rats 10 days after submission to *S. pneumoniae* meningitis and treated with RAGE or not. Data were expressed as mean \pm SEM, and

groups were compared using 2-way ANOVA and Tukey's test. * $p < 0.05$ and ** $p < 0.01$ indicate statistical significance compared to the control group; # $p < 0.05$ indicates statistical significance when compared to the meningitis group ($n = 4-5$)

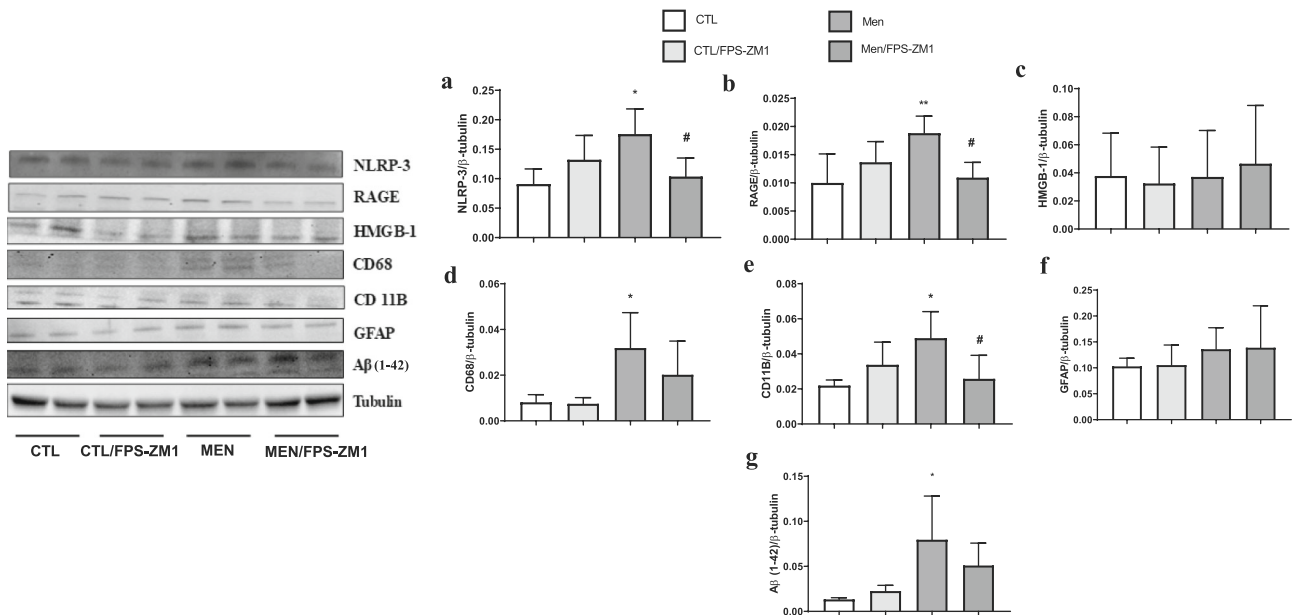


Fig. 6 Expression of NLRP3 (a), RAGE (b), HMGB1 (c), CD68 (d), CD11B (e), GFAP (f), and β -amyloid (g) in the hippocampus of Wistar rats 10 days after submission to *S. pneumoniae* meningitis and treated with RAGE or not. Data were expressed as mean \pm SEM, and groups

were compared using 2-way ANOVA and Tukey's test. * $p < 0.05$ and ** $p < 0.01$ indicate statistical significance compared to the control group; # $p < 0.05$ indicates statistical significance when compared to the meningitis group ($n = 4-5$)

expected, the RAGE inhibitor decreased $A\beta_{1-42}$ immunostaining compared to the meningitis group (Figs. 13 and 14).

Discussion

Cytokines may play a significant role in the pathogenesis of bacterial meningitis, and proinflammatory cytokines such as TNF- α , IL- β , and IL-6 are associated with poor outcomes in

bacterial meningitis. In this study, TNF- α and IL- β levels remained elevated in the PFC at 10 days after meningitis induction, corroborating our previous reports demonstrating that TNF- α levels remained higher after antibiotic treatment in the frontal cortex [29]; this increase was also associated with long-term cognitive impairment [6, 16]. In an *in vitro* study, the interaction between RAGE and its ligands induced TNF- α , IL-6, IL-1, and iNOS expression in microglial cell culture [30], and this study demonstrated that blocking

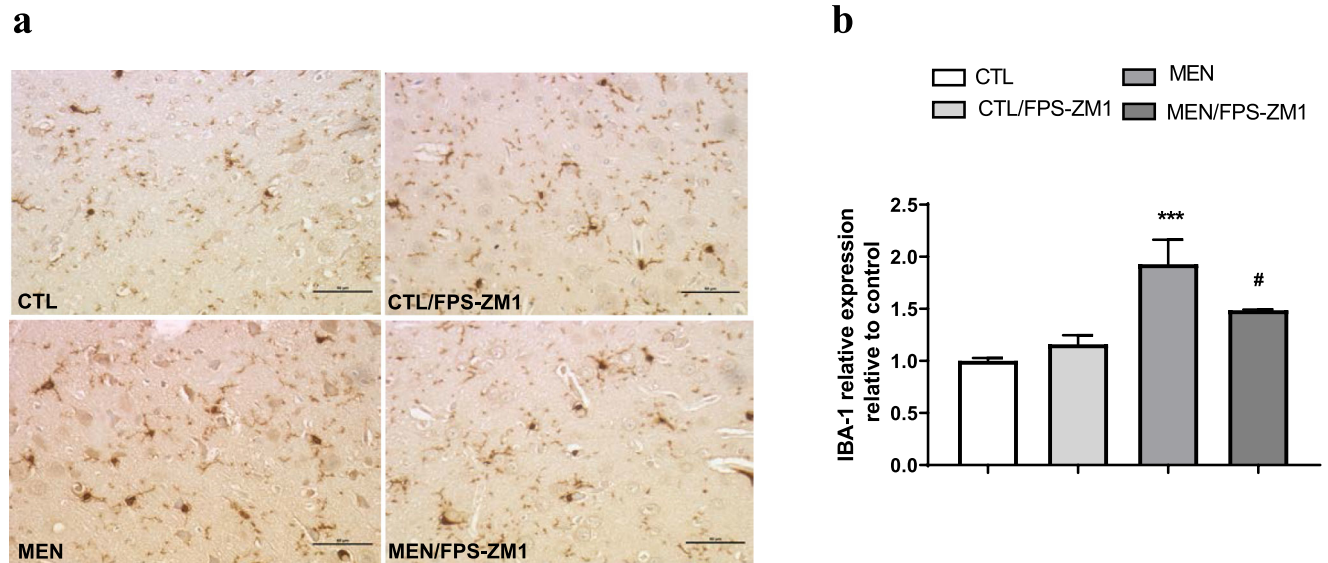


Fig. 7 Immunohistochemical staining of IBA-1 in rat brain prefrontal cortex. (a) Representative microscopic field images (magnification \times 400) immunostained with IBA-1. (b) Data are presented as the mean \pm

SEM ($n = 3-4$). *** $p < 0.0001$ as compared to the control group. # $p < 0.05$ as compared to the meningitis group

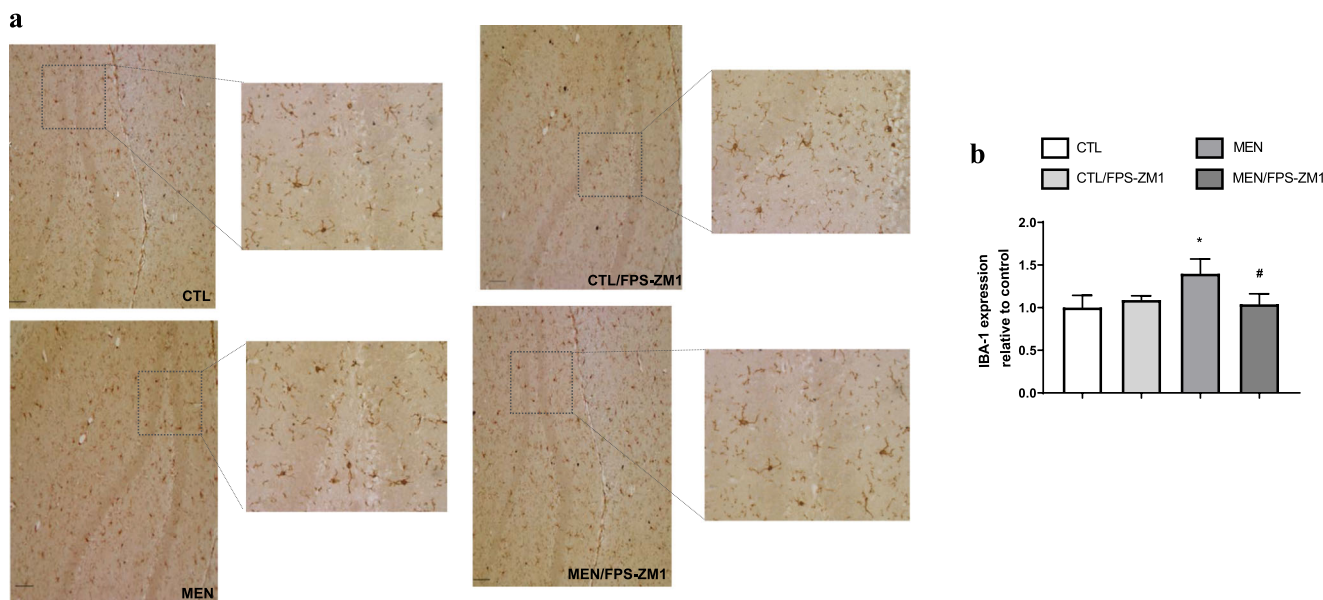


Fig. 8 Immunohistochemical staining of IBA-1 in rat brain hippocampus. (a) Representative microscopic field images (magnification $\times 100$ and $\times 400$) immunostained with IBA-1. (b) Data are presented as the mean \pm

SEM ($n = 3-4$). * $p < 0.05$ as compared to the control group. # $p < 0.05$ as compared to the meningitis group

RAGE prevented an increase in the levels of these cytokines. Brain inflammation and high levels of proinflammatory cytokines are also associated with the disruption of the BBB [31], and we demonstrated that blocking RAGE could prevent BBB disruption. Wand and collaborators found that FPS-ZM1 treatment inhibited $A\beta$ influx across the BBB and reduced the expression of RAGE, consequently decreasing hippocampal $A\beta_{1-42}$ levels in a mouse model of leptin deficiency [32]. In our study, FPS-ZM1 treatment prevented BBB disruption, reduced RAGE expression, and diminished the accumulation of $A\beta_{1-42}$ in the brains of meningitis survivor rats.

Microglial activation is a critical step in the development of brain inflammation [33]. Microglial cells are highly

specialized tissue macrophages of the CNS [34], and the dysregulation of this cell type triggers neuropsychiatric, neurodegenerative, and neuroinflammatory diseases [35]. Using positron emission tomography (PET) imaging with [^{11}C]PBR28, a radiotracer ligand that binds to 18-KDa translocator protein (TSPO), we identified *in vivo* microglia activation 10 days after meningitis induction [36]. Similarly, in this research strategy, microglia cells (IBA-1 and CD11B) were activated at 10 days after meningitis induction concomitant with an increase in RAGE and $A\beta_{1-42}$ expression in the PFC and hippocampus of meningitis survivor rats. RAGE expression intensifies microglial activation and the immune response in the brains of different experimental models, such as sepsis

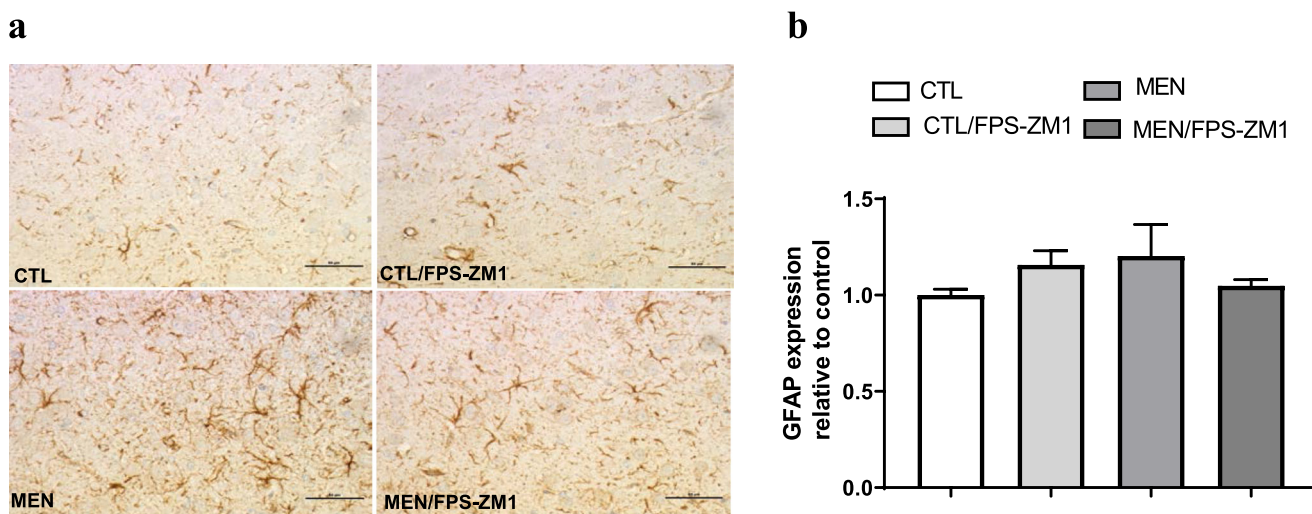


Fig. 9 Immunohistochemical staining of GFAP in rat brain prefrontal cortex. (a) Representative microscopic field images (magnification $\times 400$) immunostained with GFAP. (b) Data are presented as the mean \pm SEM ($n = 3-4$). No significant changes between groups

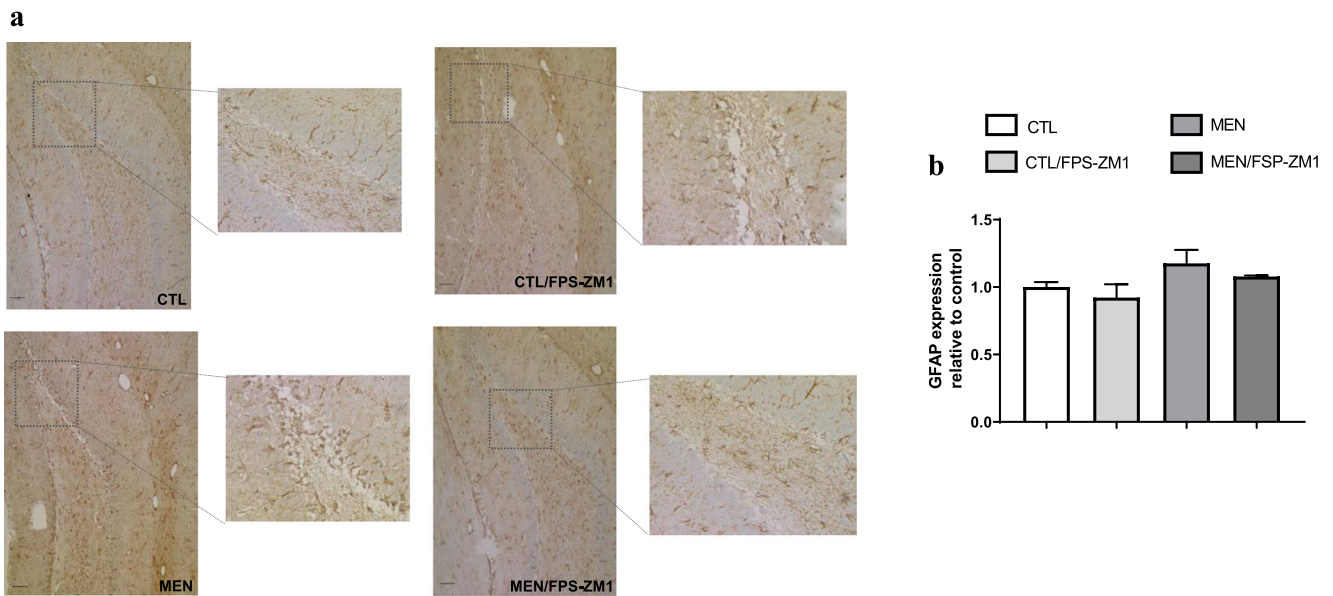


Fig. 10 Immunohistochemical staining of GFAP in rat brain hippocampus. (a) Representative microscopic field images (magnification $\times 100$ and $\times 400$) immunostained with GFAP. (b) Data are presented as the mean \pm SEM ($n = 3-4$). No significant changes between groups

[15], type 2 diabetes mellitus [32], and AD [37, 38]. However, there was no change in astrocyte expression observed as measured by GFAP expression after meningitis induction. Increasing RAGE expression can initiate several actions, such as the transport of circulating $A\beta$ into the brain; the increased production of $TNF-\alpha$, $IL-1\beta$, and $IL-6$; facilitation via immune cell trafficking across the BBB; and increased neuroinflammatory response by endothelial cells; and the onset and development of AD [39, 40]. We found that the inhibition of RAGE prevented BBB disruption in the first hours after meningitis induction, and after meningitis recovery,

RAGE inhibition by FPS-ZM1 treatment decreased RAGE and $A\beta_{1-42}$ expression, reduced cytokine levels, decreased microglial cell activation in the brain, and improved cognitive deficits in meningitis survivor rats. Similarly, in the AD mouse model, Deane et al. reported that treatment with FPS-ZM1 inhibited RAGE-mediated influx of circulating $A\beta_{40}$ and $A\beta_{42}$ into the brain. In the brain, FPS-ZM1 inhibited β -secretase activity and $A\beta$ production and suppressed microglia activation and the neuroinflammatory response [21]. In an intracerebral hemorrhage model, FPS-ZM1 treatment significantly reduced the BBB damage, brain edema, and cytokine

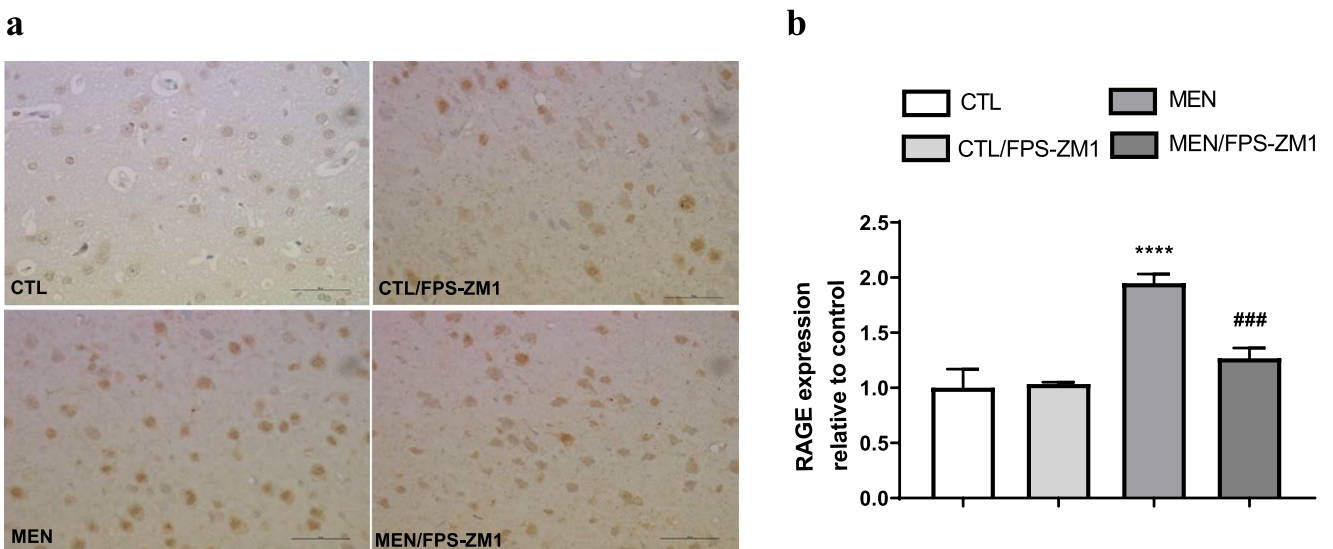


Fig. 11 Immunohistochemical staining of RAGE in rat brain prefrontal cortex. (a) Representative microscopic field images (magnification, $\times 400$) immunostained with RAGE. (b) Data are presented as the mean \pm

SEM ($n = 3-4$). **** $p < 0.0001$ as compared to the control group. ### $p < 0.001$ as compared to the meningitis group

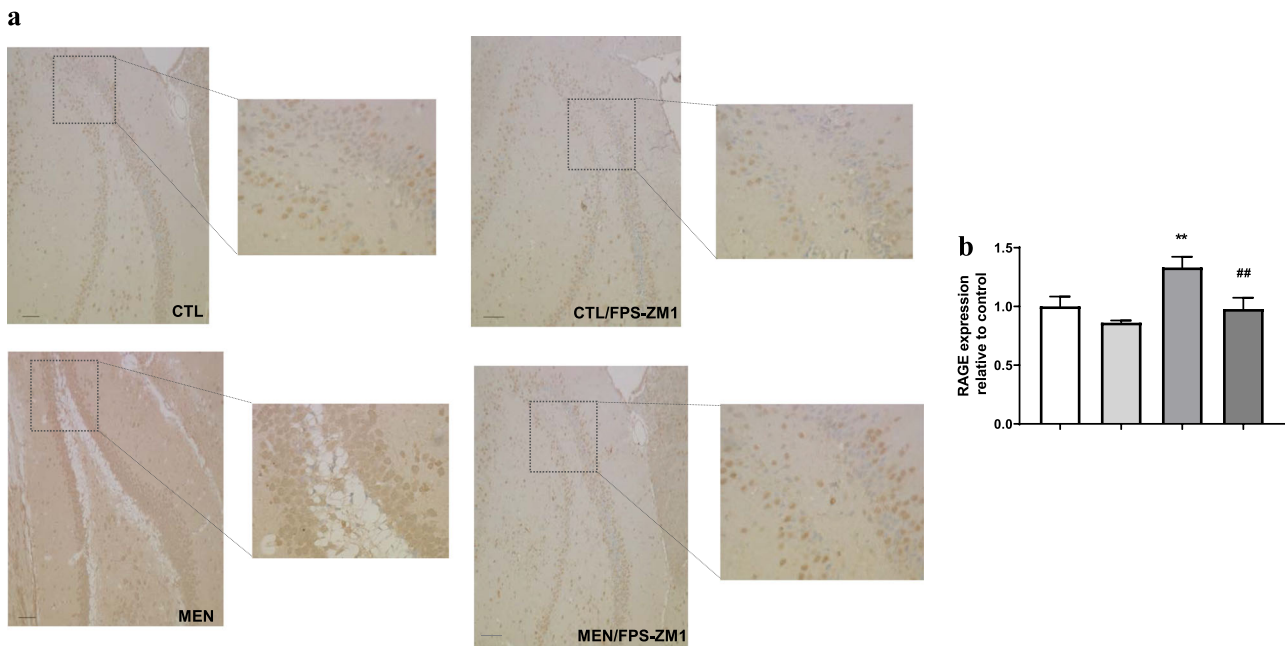


Fig. 12 Immunohistochemical staining of RAGE in rat brain hippocampus. (a) Representative microscopic field images (magnification $\times 100$ and $\times 400$) immunostained with RAGE. (b) Data are presented

as the mean \pm SEM ($n = 3-4$). $**p < 0.01$ as compared to the control group. $##p < 0.01$ as compared to the meningitis group

levels. Additionally, FPS-ZM1 demonstrated no toxic effect at 500-fold higher than its therapeutic dose of 1 mg/kg, intraperitoneally, utilized in $APP^{sw/0}$ mice. In the present study, we intraperitoneally injected 1.5 mg/kg of FPS-ZM1 for 5 days which demonstrated decreased glial activation and $A\beta$ production [41].

RAGE mediates $A\beta$ -induced perturbations in the BBB, neurons, and microglia in AD [21], in which sporadic onset accounts for 95% of cases [42]. The infection has the potential to play a role in sporadic cases of AD [43]. *Salmonella*

serotype Typhimurium injected into the brains of transgenic 5XFAD mice resulted in the fast deposition of $A\beta$ colocalized with invading bacteria [44]. In experimental sepsis, RAGE, $A\beta$, and microglia markers were increased in the wild-type rat brain. Despite sepsis triggering brain inflammation and cognitive impairment, the intracerebral injection of RAGE antibody into the hippocampus reduced $A\beta$ accumulation, decreased RAGE expression and microglial cell activation, and prevented behavioral deficits evaluated by the inhibitory avoidance and novel object recognition tasks associated with

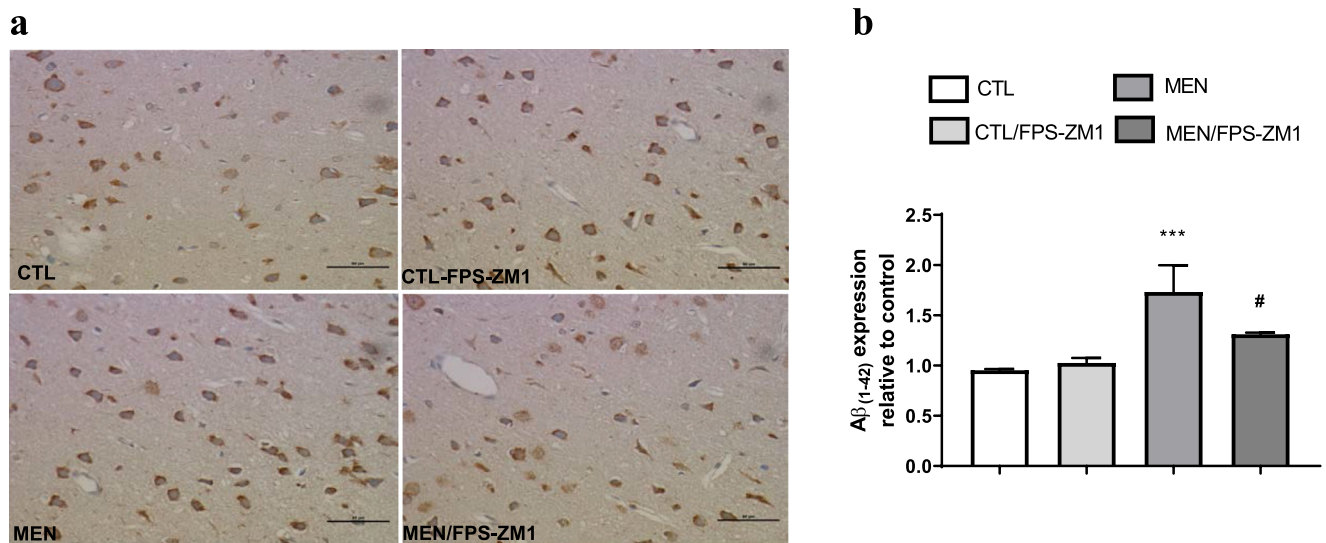


Fig. 13 Immunohistochemical staining of $A\beta_{1-42}$ in rat brain prefrontal cortex. (a) Representative microscopic field images (magnification $\times 400$) immunostained with $A\beta_{1-42}$. (b) Data are presented as the mean \pm SEM

($n = 3-4$). $***p < 0.001$ as compared to the control group. $#p < 0.05$ as compared to the meningitis group

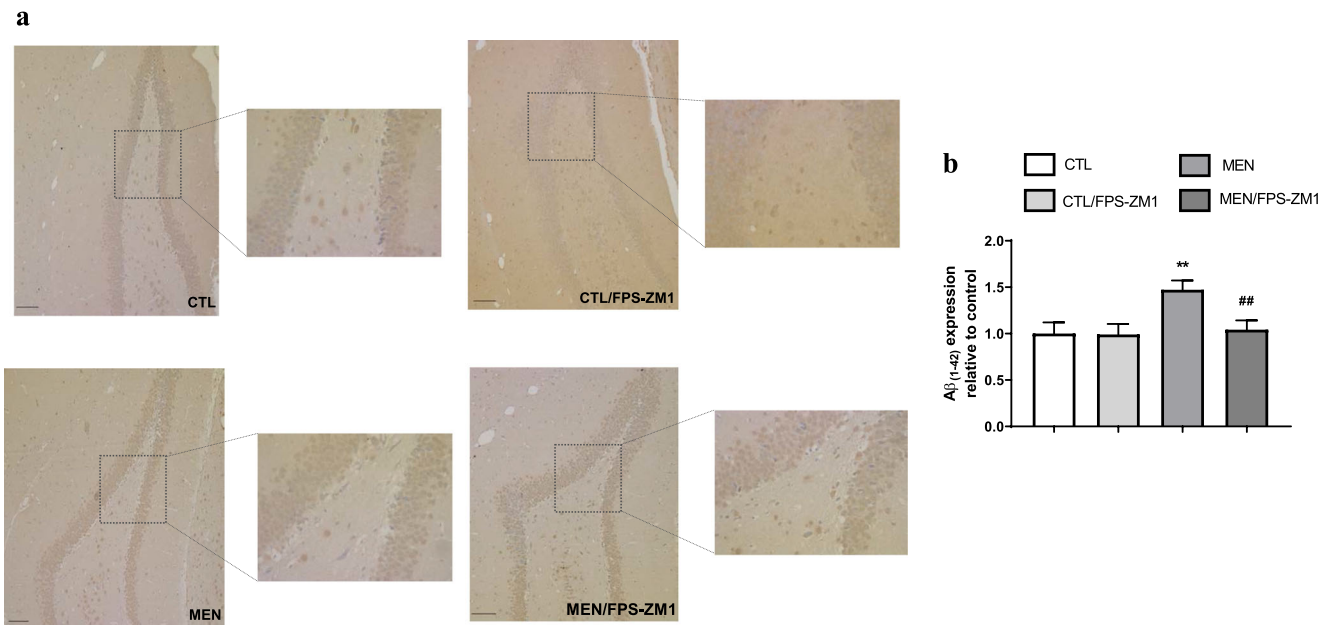


Fig. 14 Immunohistochemical staining of A β_{1-42} in rat brain hippocampus. (a) Representative microscopic field images (magnification $\times 100$ and $\times 400$) immunostained with A β_{1-42} . (b) Data are presented

as the mean \pm SEM ($n = 3-4$). ** $p < 0.01$ as compared to the control group. ## $p < 0.01$ as compared to the meningitis group

cognitive impairment in sepsis survivors [15]. In our study, we also verify that the RAGE inhibition improved recognition memory, habituation memory, and spatial memory as measured by the novel object recognition task, open-field task, and MWM task, respectively, by using separate cohorts of animals. Although there is no difference between the groups during the training trial, the probe trial demonstrated a significant difference between meningitis and control rats. The RAGE inhibitor-treated rats spent more in the target quadrant. In the AD transgenic mice model, APP/PS1, the RAGE inhibition by the blocking RAGE/A β axis improved cognitive deficits evaluate by MWM [45].

The possibility is that A β acts as an antimicrobial peptide, and the pathogen triggers A β production and deposition in the brain, starting with the pathological cascade associated with AD [46]. Other studies also support the hypothesis of the role of infectious agents in AD pathology, such as *Porphyromonas gingivalis* [47], *Toxoplasma gondii* [48], and herpes simplex virus type 1 (HSV-1) [49] infections. The inflammatory hypothesis has recently been reinforced by genome-wide association studies that identified genes for immune receptors, triggering receptors expressed on myeloid cells-2 (TREM-2) [50] and CD33 [51], which are associated with an increased risk of AD. We also observed increased levels of the inflammasome (NLRP-3 expression) and CD68 markers in meningitis survivors as compared to the control group. Regardless of the cause, this sequence of events generated by pneumococcal meningitis persists long after the resolution of the infection and recovery; however, these events can trigger a neurocognitive decline. The RAGE–A β axis is a common feature underlying many infections and neurodegenerative diseases.

A better understanding of this critical mechanism may help prevent cognitive impairment in patients who are survivors of infectious diseases.

Conclusion and Future Perspectives

In this study, we demonstrated that experimental pneumococcal meningitis increased RAGE and A β expression, triggered BBB disruption, caused microglial cell activation, and resulted in cognitive impairment in experimental meningitis. Targeted RAGE inhibition by FPS-ZM1 was able to reduce cytokine levels, decrease the expression levels of A β_{1-42} , inhibit microglial cell activation, and improve cognitive deficits in meningitis survivor rats. Future directions should replicate these data using an AD mouse model subjected to meningitis.

Acknowledgments This work was supported by the Faillace Department of Psychiatry and Behavioral Sciences, McGovern Medical School, The University of Texas Health Science Center at Houston (UTHealth), USA (TB, VVG, and RH); the Graduate Program in Health Sciences, University of Southern Santa Catarina (UNESC) (TB, FDP, JSG, DD, and AC), Brazil, and the Alzheimer's Association Grant number AARGDNTF-19-619645 (TB).

Required Author Forms Disclosure forms provided by the authors are available with the online version of this article.

Compliance with Ethical Standards

Conflict of Interest The authors declare that they have no conflicts of interest.

References

- Bijlsma MW, Brouwer MC, Kasanmoentalib ES, et al. Community-acquired bacterial meningitis in adults in the Netherlands, 2006-14: a prospective cohort study. *Lancet Infect Dis* 2016;16(3):339-347.
- Johnson AP, Waight P, Andrews N, Pebody R, George RC, Miller E. Morbidity and mortality of pneumococcal meningitis and serotypes of causative strains prior to introduction of the 7-valent conjugant pneumococcal vaccine in England. *J Infect* 2007;55(5):394-399.
- Oligbu G, Collins S, Djennad A, et al. Effect of pneumococcal conjugate vaccines on pneumococcal meningitis, England and Wales, July 1, 2000-June 30, 2016. *Emerg Infect Dis* 2019;25(9):1708-1718.
- Buchholz G, Koedel U, Pfister HW, Kastenbauer S, Klein M. Dramatic reduction of mortality in pneumococcal meningitis. *Crit Care*. 2016;20(1):312.
- Jit M. The risk of sequelae due to pneumococcal meningitis in high-income countries: a systematic review and meta-analysis. *J Infect* 2010;61(2):114-124.
- Barichello T, Generoso JS, Simoes LR, Elias SG, Quevedo J. Role of oxidative stress in the pathophysiology of pneumococcal meningitis. *Oxidative Med Cell Longev* 2013;2013:371465.
- Tatiana Barichello AC, Hasbun R, Morales R. An overview of the blood-brain barrier in The Blood-Brain Barrier Protocols. *Spring Nature Protocols*. 2019;1 (ISBN 978-1-4939-8946-1):8
- Mook-Kanamori BB, Geldhoff M, van der Poll T, van de Beek D. Pathogenesis and pathophysiology of pneumococcal meningitis. *Clin Microbiol Rev* 2011;24(3):557-91.
- Gong T, Liu L, Jiang W, Zhou R. DAMP-sensing receptors in sterile inflammation and inflammatory diseases *Nat Rev Immunol*. 2019
- Franklin TC, Wohleb ES, Zhang Y, Fogaca M, Hare B, Duman RS. Persistent increase in microglial RAGE contributes to chronic stress-induced priming of depressive-like behavior. *Biol Psychiatry* 2018;83(1):50-60.
- Kim J, Waldvogel HJ, Faull RL, Curtis MA, Nicholson LF. The RAGE receptor and its ligands are highly expressed in astrocytes in a grade-dependant manner in the striatum and subependymal layer in Huntington's disease. *J Neurochem* 2015;134(5):927-942.
- Deane R, Du Yan S, Subramanyam RK, et al. RAGE mediates amyloid-beta peptide transport across the blood-brain barrier and accumulation in brain. *Nat Med* 2003;9(7):907-913.
- Takuma K, Fang F, Zhang W, et al. RAGE-mediated signaling contributes to intraneuronal transport of amyloid-beta and neuronal dysfunction. *Proc Natl Acad Sci U S A* 2009;106(47):20021-20026.
- Hudson BI, Lippman ME. Targeting RAGE Signaling in Inflammatory Disease. *Annu Rev Med* 2018;69:349-364.
- Gasparotto J, Girardi CS, Somensi N, et al. Receptor for advanced glycation end products mediates sepsis-triggered amyloid-beta accumulation, Tau phosphorylation, and cognitive impairment. *J Biol Chem* 2018;293(1):226-244.
- Barichello T, Generoso JS, Simoes LR, et al. Inhibition of indoleamine 2,3-dioxygenase prevented cognitive impairment in adult Wistar rats subjected to pneumococcal meningitis. *Transl Res* 2013;162(6):390-397.
- Mahat MY, Fakrudeen Ali Ahamed N, Chandrasekaran S, Rajagopal S, Narayanan S, Surendran N. An improved method of transcutaneous cisterna magna puncture for cerebrospinal fluid sampling in rats. *J Neurosci Methods* 2012;211(2):272-279.
- Lebedev SV, Blinov DV, Petrov SV. Spatial characteristics of cisterna magna in rats and novel technique for puncture with a stereotaxic manipulator. *Bull Exp Biol Med* 2004;137(6):635-8.
- Simoes LR, Abreu R, Generoso JS, et al. Prevention of Memory Impairment and Neurotrophic Factors Increased by Lithium in Wistar Rats Submitted to Pneumococcal Meningitis Model. *Mediat Inflamm* 2017;2017:6490652.
- Barichello T, Goncalves JC, Generoso JS, et al. Attenuation of cognitive impairment by the nonbacteriolytic antibiotic daptomycin in Wistar rats submitted to pneumococcal meningitis. *BMC Neurosci* 2013;14:42.
- Deane R, Singh I, Sagare AP, et al. A multimodal RAGE-specific inhibitor reduces amyloid beta-mediated brain disorder in a mouse model of Alzheimer disease. *J Clin Invest* 2012;122(4):1377-1392.
- Smith SL, Hall ED. Mild pre- and posttraumatic hypothermia attenuates blood-brain barrier damage following controlled cortical impact injury in the rat. *J Neurotrauma* 1996;13(1):1-9.
- Vianna MR, Alonso M, Viola H, et al. Role of hippocampal signaling pathways in long-term memory formation of a nonassociative learning task in the rat. *Learn Mem* 2000;7(5):333-340.
- Morris R. Developments of a water-maze procedure for studying spatial learning in the rat. *J Neurosci Methods* 1984;11(1):47-60.
- Lowry OH, Rosebrough NJ, Farr AL, Randall RJ. Protein measurement with the Folin phenol reagent. *J Biol Chem* 1951;193(1):265-275.
- Dandekar MP, Luse D, Hoffmann C, Cotton P, Peery T, Ruiz C, et al. Increased dopamine receptor expression and anti-depressant response following deep brain stimulation of the medial forebrain bundle. *J Affect Disord* 2017;217:80-88.
- Barichello T, Generoso JS, Michelon CM, et al. Inhibition of matrix metalloproteinases-2 and -9 prevents cognitive impairment induced by pneumococcal meningitis in Wistar rats. *Exp Biol Med (Maywood)*. 2014;239(2):225-231.
- Barichello T, Generoso JS, Simoes LR, et al. Sodium butyrate prevents memory impairment by re-establishing BDNF and GDNF expression in experimental pneumococcal meningitis. *Mol Neurobiol* 2015;52(1):734-740.
- Barichello T, Milioli G, Generoso JS, et al. Imipramine reverses depressive-like parameters in pneumococcal meningitis survivor rats. *J Neural Transm (Vienna)*. 2012;119(6):653-660.
- Dukic-Stefanovic S, Gasic-Milenkovic J, Deuther-Conrad W, Munch G. Signal transduction pathways in mouse microglia N-11 cells activated by advanced glycation endproducts (AGEs). *J Neurochem* 2003;87(1):44-55.
- Yau B, Hunt NH, Mitchell AJ, Too LK. Blood brain barrier pathology and CNS outcomes in *Streptococcus pneumoniae* meningitis. *Int J Mol Sci*. 2018;19(11).
- Wang H, Chen F, Du YF, et al. Targeted inhibition of RAGE reduces amyloid-beta influx across the blood-brain barrier and improves cognitive deficits in db/db mice. *Neuropharmacology* 2018;131:143-153.
- Shigemoto-Mogami Y, Hoshikawa K, Sato K. Activated microglia disrupt the blood-brain barrier and induce chemokines and cytokines in a rat in vitro model. *Front Cell Neurosci* 2018;12:494.
- Priller J, Prinz M. Targeting microglia in brain disorders. *Science (New York, NY)*. 2019;365(6448):32-3.
- Kierdorf K, Prinz M. Microglia: same same, but different. *J Exp Med* 2019
- Giridharan VV, Collodel A, Generoso JS, et al. Neuroinflammation trajectories precede cognitive impairment after experimental meningitis-evidence from an in vivo PET study. *J Neuroinflammation*. 2020;17(1):5-.
- Fang F, Yu Q, Arancio O, et al. RAGE mediates Abeta accumulation in a mouse model of Alzheimer's disease via modulation of beta- and gamma-secretase activity. *Hum Mol Genet* 2018;27(6):1002-1014.
- Batkulwar K, Godbole R, Banarjee R, Kassar O, Williams RJ, Kulkarni MJ. Advanced glycation end products modulate amyloidogenic APP processing and tau phosphorylation: a

- mechanistic link between glycation and the development of Alzheimer's disease. *ACS Chem Neurosci* 2018;9(5):988-1000.
39. Sagare AP, Bell RD, Zlokovic BV. Neurovascular dysfunction and faulty amyloid beta-peptide clearance in Alzheimer disease. *Cold Spring Harb Perspect Med.* 2012;2(10).
 40. Pugazhenti S, Qin L, Reddy PH. Common neurodegenerative pathways in obesity, diabetes, and Alzheimer's disease. *Biochim Biophys Acta Mol basis Dis* 2017;1863(5):1037-1045.
 41. Yang F, Wang Z, Zhang JH, et al. Receptor for advanced glycation end-product antagonist reduces blood-brain barrier damage after intracerebral hemorrhage. *Stroke* 2015;46(5):1328-1336.
 42. Bakhta K, Cecillon E, Lacombe E, Lamy M, Leboucher A, Philippe J. Alzheimer's disease and neurodegenerative diseases in France. *Lancet.* 2019;394(10197):466-467.
 43. Giridharan VV, Masud F, Petronilho F, Dal-Pizzol F, Barichello T. Infection-induced systemic inflammation is a potential driver of Alzheimer's disease progression. *Front Aging Neurosci* 2019;11:122.
 44. Kumar DK, Choi SH, Washicosky KJ, et al. Amyloid-beta peptide protects against microbial infection in mouse and worm models of Alzheimer's disease. *Sci Transl Med.* 2016;8(340):340ra72.
 45. Cui L, Cai Y, Cheng W, et al. A novel, multi-target natural drug candidate, matrine, improves cognitive deficits in Alzheimer's disease transgenic mice by inhibiting A β aggregation and blocking the RAGE/A β axis. *Mol Neurobiol* 2017;54(3):1939-1952.
 46. Golde TE. Alzheimer disease: host immune defence, amyloid-beta peptide and Alzheimer disease. *Nat Rev Neurol* 2016;12(8):433-434.
 47. Dominy SS, Lynch C, Ermini F, et al. Porphyromonas gingivalis in Alzheimer's disease brains: evidence for disease causation and treatment with small-molecule inhibitors. *Sci Adv.* 2019;5(1):eaau3333.
 48. Torres L, Robinson SA, Kim DG, Yan A, Cleland TA, Bynoe MS. Toxoplasma gondii alters NMDAR signaling and induces signs of Alzheimer's disease in wild-type, C57BL/6 mice. *J Neuroinflammation* 2018;15(1):57.
 49. De Chiara G, Piacentini R, Fabiani M, et al. Recurrent herpes simplex virus-1 infection induces hallmarks of neurodegeneration and cognitive deficits in mice. *PLoS Pathog* 2019;15(3):e1007617.
 50. Guerreiro R, Wojtas A, Bras J, et al. TREM2 variants in Alzheimer's disease. *N Engl J Med* 2013;368(2):117-627.
 51. Griciuc A, Serrano-Pozo A, Parrado AR, et al. Alzheimer's disease risk gene CD33 inhibits microglial uptake of amyloid beta. *Neuron* 2013;78(4):631-643.

Publisher's Note Springer Nature remains neutral with regard to jurisdictional claims in published maps and institutional affiliations.